DOI: http://dx.doi.org/10.22104/ijhfc.2014.95

Iranian Journal of Hydrogen & Fuel Cell 3(2014) 175-188

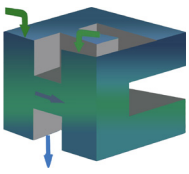

Iranian Journal of Hydrogen & Fuel Cell

IJHFC

Journal homepage://ijhfc.irost.ir

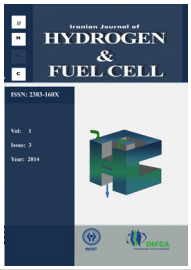

The simulation of novel annular shape on the performance in proton exchange membrane fuel cell

N. Pourmahmoud[1], A.Torkavannejad[*,2]

[1] **mechanical department, Urmia University, Postal Code 57561-15311,Urmia**
[2] **mechanical department, Urmia University Postal Code 57561-15311,Urmia**

Article Information

Article History:

Received:
19 November 2014
Received in revised form:
27 January 2015
Accepted:
24 February 2015

Keywords

Fuel cell performance
PEM fuel cells
Single-phase
Annular geometry

Abstract

In this article, one-phase and three dimensional computational fluid dynamics analysis was utilized to investigate the effect of annular field pattern of proton exchange membrane fuel cells (PEMFC) with different geometry on the performances and species distribution. This computational fluid dynamics code is used for solving the equation in single domain namely the flow field, the mass conservation, the energy conservation, the species transport, and the electric/ionic fields under the assumptions of steady state and non-isothermal. The introduced cell consist of different novelties, such as the way in which reactant gases are supplied to the flow field, the design of the flow field geometry for both anode and cathode and the membrane electrode assembly design and the length and occupied volume decreases up to 40%. Obtained results showed that generation of fuel cells with annular shaped geometry with the same active area and inlet area gave intensively higher current density compared with conventional model. Oxygen, hydrogen and water mass fraction distributions, current density and temperature distribution has been studied. The main factors that affect the behavior of each of the curves are discussed comprehensively. Intorduced configuration allows for better flow distribution and uses of the maximum active area and diffusion from two side in each channels. Furthermore, the effect of changing the GDL thickness is presented in order to understand the effect of different parameters. Simulation results were compared with the experimental data and confirm the accuracy of model.

1. Introduction

In recent years, researchers pay more attention on reliable, clean and safer energy sources. Their study concentrate on industrialization and optimization of this energy systems.one of the most attractive and distinguished power sources is proton exchange membrane fuel cell (PEMFC). PEM fuel cells have been considered as a principle power sources for transportation application and small scale systems as well as for small devices such as laptop, mobile. Optimization of these systems for commercial

[*]Corresponding author: E-mail address: a.torkavannejad@yahoo.com (A. Torkavannejad)

using is great challenge for the researchers. In this regard, a lot of optimization has been done on the PEM fuel cell in order to enhance efficiency of such systems. Novel geometries and architectures of PEM fuel cell have been explored to improve the efficiency and solve technical problems such as species transportation, water flooding, misdistribution and non-uniformity of current density. Among a lot of parameters which affect the performance, design of flow field and the way of supplying and distribution of reactants has striking effect on the fuel cell performances.

Therefore, many works have focused on this important task. Nader pourmahmoud worked on the geometries and different channel configuration in order to increase performance of PEM fuel cell geometries [1-6]. Wang et al. [7] used baffle in serpentine channel which result showed at low operating voltage, the cell performance increased. They also optimized the serpentine pattern with varying the channel heights for better distribution [8]. Alvarado et al. [9] worked on serpentine symmetric flow pattern which leads to improve power generation. Chen et.al [10] investigated on novel flow field as z-type and interdigited channels.

In the previous years, researcher study on alternative for conventional geometry. A lot of new geometries have been simulated and fabricated like radial and spiral flow PEMFCs for the sake of performance enhancement due to increment of reaction area along the length of the channel [11-15]. Tiss et al. [16] designed several blocks along the channel to force reactants in the gas distribution. The results showed this model improve the output current density. Walckzy et al. [17] investigate on ribbon architecture. Even current distribution, lower fuel cell cost, easy removal of product water.

M. Khazaee [18] introduced annular and duct-shaped PEMFC which is fundamentally different architecture. Moreover, His works is the one off the innovative simulation to progress in the architecture of the future PEMFC .

In the present study, three-dimensional, single phase, non-isothermal and parallel flow model of a PEM fuel cell with annular channel with novel MEA and channel geometry was conducted which every channel is in connection with two membrane assembly for more diffusion and improvement of reaction area. These geometries were used same boundary conditions and inlet area and including fully humidification for both anode and cathode. The goal of this article is to design novel geometry to improve the reactant distribution and improve the cell performance and study different parameters. The simulation results were verified by comparison with results in the literature and showed good concord with experimental data. Comprehensive analyses of the fuel cell behavior under this generation of geomerty are discussed in the following sections.

2. Model description

2.1 System description

Constant mass flow rate at the channel, inlet constant pressure condition at the channel outlet, and no-flux conditions are executed for mass, momentum, species and potential conservation equations at all boundaries except for inlets and outlets of the anode and cathode flow channels. The side's faces are symmetrical.

Figure 1 indicates the traditional domain of base model and table 1 shows the Geometric parameters and operation conditions for base model. The cell consists of hydrogen and oxygen channels, bipolar plates on cathode and anode side of cell, which act as current collector with high electronic conductivity and the membrane electrode assembly (MEA) is located between gas channels.

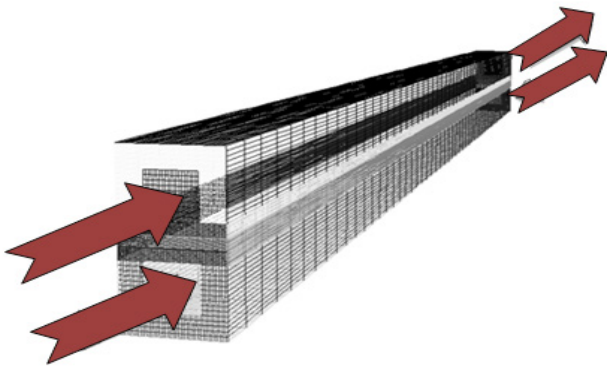

Fig. 1. Computational domain of base model.

Table 1. Geomerric paramets and operation conditions for base model.

Parameter	Symbol	Value	Unit
Channel length	L	0.05	m
Channel width	W	1e_3	m
Channel height	H	1e_3	m
Land area width	Wland	1e_3	m
Gas diffusion layer thickness	dGDL	0.26e_3	m
Wet membrane thickness (Nafion 117)	mem		
0.23e_3	m $\hat{o}$		
Catalyst layer thickness	CL $\hat{o}$		
0.0287e_3	m		
Anode pressure	Pa	3	atm
Cathode pressure	Pc	3	atm
Inlet fuel and air temperature	Tcell	353.15	K
Relative humidity of inlet fuel and air (fully humidified conditions)	ψ	100	%
Refrence current density	I	10	A/cm^2
Inlet anode oxygen mass fraction	YOXYGEN,A	0	-
Inlet anode hydrogen mass fraction	YHYDROGEN,A	0.3780066	-
Inlet anode water mass farction	YWATER,A	0.6219934	-
Inlet cathode water mass fraction	YWATER,C	0.1031307	-
Inlet cathode oxygen mass fraction	YOXYGEN,C	0.2088548	-
Inlet cathode hydrogen mass fraction	YHYDROGEN,C	0	-
Membrane equivalent weight	-	1.1	Kg/mol

Figure 2 and 3 show the configuration of the proposed fuel cell. This fuel cell has the same active and operation condition which the base fuel has, in order to compare the result. The reactant gases are supplied from inlet channels and leaved by the area formed in the outer edge of the cell. As it is obvious in the figure, every cathode flow field is in contact with two anode reaction area and vice versa. This new geometry is very unique and novel due to its geometry and performance. The geometric parameters are presented Table 2.

Table 2. Geometric parametrs for simplifie model (single cell).

INLET CHANNEL WIDTH	0.8 mm
OUTLET CHANNEL WIDTH	0.8 mm
SHOULDER WIDTH	0.25 mm
Cell LENGTH	25mm
GAS DIFFUSION LAYER THICKNESS	0.26 mm
CATALYST LAYER THICKNESS	0.0287mm
MEMBRANE THICKNESS	0.23mm

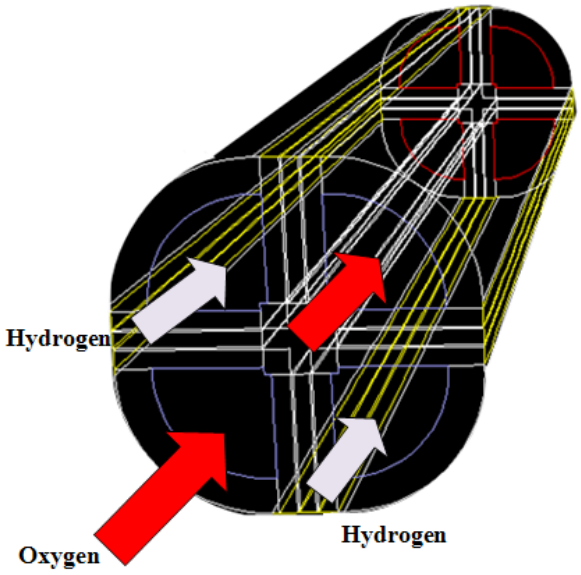

Fig. 2. Schematic of the annular fuel cell

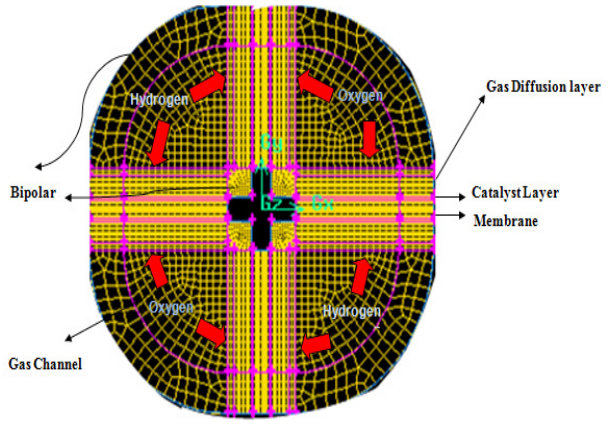

Fig. 3. Simplified model of the novel fuel cell.

2.2 Model assumption

The model aims to study the electrochemical kinetics, current distribution, reactant flow fields and multi-component transport of oxidizer and fuel streams in a multi-dimensional domain. The model is built considering the following assumptions:

• Non-isothermal model is assumed to perform in steady manner under constant load conditions.

• All gases are assumed to obey ideal gas behaviors.

• Gas diffusion layer and catalyst layers are homogeneous and isotropic porous mediums.

• Flow is incompressible and laminar due to the low pressure gradients and velocities.

• Volume of liquid-phase water produced in electrochemical reactions is negligible and phase change or two phase-transports are not considered so this model is considered as a single phase.

• The membrane is impermeable to cross-over of reactant gases and assumed to be fully humidified.

• The species diffusion and electrochemical reaction conform to the dilute solution theory and Butler-Volmer kinetic equation respectively.

• The fully humidified inlet condition for anode and cathode is used.

3. Model equations

3.1. Gas flow fields

In the fuel cell, the gas-flow field is obtained by solving the steady-state Navier-Stokes equations, i.e. the continuity equation:

$$\nabla.\left(\rho u\right)=0 \tag{1}$$

and momentum equations;

$$\nabla.\left(\rho u\otimes u-\mu\nabla u\right)= -\nabla\left(P+\frac{2}{3}\mu\nabla u\right)+\nabla.\left[\mu\left(\nabla u\right)^{T}\right] \tag{2}$$

The mass balance is described by the divergence of the mass flux through diffusion and convection. The steady state mass transport equation can also be written in the following expression for species i:

$$\nabla.\left[-\rho y_i\sum_{j=1}^{M}D_{ij}\frac{M}{M_j}\left(\nabla y_j+\frac{\nabla M}{M}\right)+\rho y_i u\right]=0 \tag{3}$$

where the subscript i denotes oxygen at the cathode side, and hydrogen at the anode side, and j is water vapor in both cases. Nitrogen is the third species at the cathode side.

The Maxwell-Stefan diffusion coefficients of any two species are dependent on temperature and pressure. They can be calculated according to the empirical relation based on the kinetic gas theory [19];

$$D_{ij}=\frac{T^{1.75}\times10^{-3}}{P\left[\left(\sum_k V_{ki}\right)^{1/3}+\left(\sum_k V_{kj}\right)^{1/3}\right]^2}\left[\frac{1}{M_i}+\frac{1}{M_j}\right]^{1/2} \tag{4}$$

In this equation, pressure is in [bar], and the binary diffusion coefficient is in [cm^2/s]. The values for $\sum V_{ki}$ are given by Fuller et al., and the temperature field is obtained by solving the convective energy equation;

$$\nabla.\left(\rho C_P u T-k\nabla T\right)=0 \tag{5}$$

3.2. Gas diffusion layers

Transport in the gas diffusion layer is modeled as transport in a porous media. The continuity equation in the gas diffusion layers becomes:

$$\nabla.\left(\rho\varepsilon u\right)=0 \tag{6}$$

The momentum equation reduces to Darcy's law:

$$u=\frac{K_p}{\mu}\nabla P \tag{7}$$

The mass transport equation in porous media is:

$$\nabla.\left[-\rho\varepsilon y_i\sum_{j=1}^{M}D_{ij}\frac{M}{M_j}\left(\nabla y_i+y_i\frac{\nabla M}{M}\right)+\rho\varepsilon y_i u\right]=0 \tag{8}$$

In order to account for geometric constraints of the porous media, the diffusivities are corrected using the Bruggemann correction formula:

$$D_{ij}^{eff}=D_{ij}\times\varepsilon^{1.5} \tag{9}$$

The heat transfer in the gas diffusion layers is governed by:

$$\nabla.\left(\rho\varepsilon Cpu T-k_{eff}\varepsilon\nabla T\right)=\varepsilon\beta\left(T_{solid}-T\right) \tag{10}$$

where, the term on the right-hand side accounts for the heat exchange to and from the solid matrix of the GDL. Here, β is a modified heat transfer coefficient that accounts for the convective heat transfer in [W/m^2] and the specific surface area [m^2/m^3] of the porous medium. Hence, the unit of β is [W/m^3]. The potential distribution in the gas diffusion layers is:

$$\nabla.\left(\lambda_e\nabla\phi\right)=0 \tag{11}$$

3.3. Catalyst layers

The catalyst layer is treated as a thin interface, where sink and source terms for the reactants are implemented. Due to the infinitesimal thickness, the source terms are actually implemented in the last grid cell of the porous medium. At the cathode side, the sink term for oxygen can be written as:

$$S_{O_2}=-\frac{M_{O_2}}{4F}i_c \tag{12}$$

Whereas, the sink term for hydrogen is specified as:

$$S_{H_2}=-\frac{M_{H_2}}{4F}i_a \tag{13}$$

The production of water is modeled as a source terms and hence can be given as:

$$S_{H_2O}=-\frac{M_{H_2O}}{2F}i_c \tag{14}$$

The generation of heat in the cell is due to entropy changes as well as irreversibility due to the activation overpotential:

$$\dot{q}=\left[\frac{T\left(-\nabla s\right)}{n_eF}+\eta_{act,c}\right]i_c \tag{15}$$

The local current density distribution in the catalyst layers can be modeled by the Butler-Volmer equation:

$$i_c=i_{o,c}^{ref}\left(\frac{C_{O_2}}{C_{O_2}^{ref}}\right)\left[\exp\left(\frac{\alpha_aF}{RT}\eta_{act,c}\right)+\exp\left(-\frac{\alpha_cF}{RT}\eta_{act,c}\right)\right] \tag{16}$$

$$i_a=i_{o,a}^{ref}\left(\frac{C_{H_2}}{C_{H_2}^{ref}}\right)^{0.5}\left[\exp\left(\frac{\alpha_aF}{RT}\eta_{act,a}\right)+\exp\left(-\frac{\alpha_cF}{RT}\eta_{act,a}\right)\right] \tag{17}$$

3.4. Membrane

The balance between the electro-osmotic drag of water from anode to cathode and back diffusion from cathode to anode yields the net water flux through the membrane:

$$N_W=n_dM_{H_2O}\frac{i}{F}-\nabla\left(\rho D_w\nabla y_w\right) \tag{18}$$

For heat transfer purposes, the membrane is considered a conducting solid, which means that the transfer of energy associated with the net water flux through the membrane is neglected. Heat transfer in the membrane is governed by:

$$\nabla.\left(k_{mem}\nabla T\right)=0 \quad (19)$$

$$\nabla.\left(\lambda_{m}\nabla \phi\right)=0 \quad (20)$$

3.5. Boundary conditions

For the momentum conservation equation, fuel velocity is specified at each inlet of anode and cathode flow channel. The velocity is calculated based on the concept of stoichiometry, which means "the required amount of fuel at a given condition". Boundary conditions are set as follows: constant mass flow rate at the channel inlet and constant pressure condition at the channel outlet which means it discharges to the atmosphere. The inlet mass fractions are determined by the inlet pressure and humidity according to the ideal gas law. Gradients at the channel exits are set to zero. The equations for both inlets are expressed as:

$$\left|\vec{u}\right|_{in}=\frac{\zeta}{X_{H_{2,in}}}\frac{I_{avg}}{2F}\frac{RT_{in}}{P_{in}}\frac{A_{MEA}}{A_{ch}}$$

I_{avg} is the average current density at a given cell-potential. Where, R, T_{in}, P_{in}, and ζ are the universal gas constant, temperature in the inlet, pressure in the inlet, and stoichiometric ratio respectively. The later is defined as the ratio between the amount of supplied and the amount of required reactant on the basis of the reference current density I_{avg}, accordingly. The model parameter values are given in Tables 1 and 2, and the inlet conditions are shown in Table 1.

4. Numerical implementations

For solving the equations, the computational fluid dynamic codes are utilized by applying finite volume scheme and simple algorithm. Figure 4 shows the algorithm (SIMPLE).

The grid independence test results were performed to ensure that the solutions were independent of the grid size. Moreover, the computational domain is divided into about 164000 unstructured cells to minimize the numbers of iteration and maximize the accuracy. The number of calculation was used as 800 for low current output and 1200 for high current density and the criterion convergence between accurate iterations is less than 10^{-7} for all variables. An IBM-PC-Pentium 5 (CPU speed is 2.4 GHz) was determined to solve the set of equations. The computational time for solving the set of equations was 6 h.

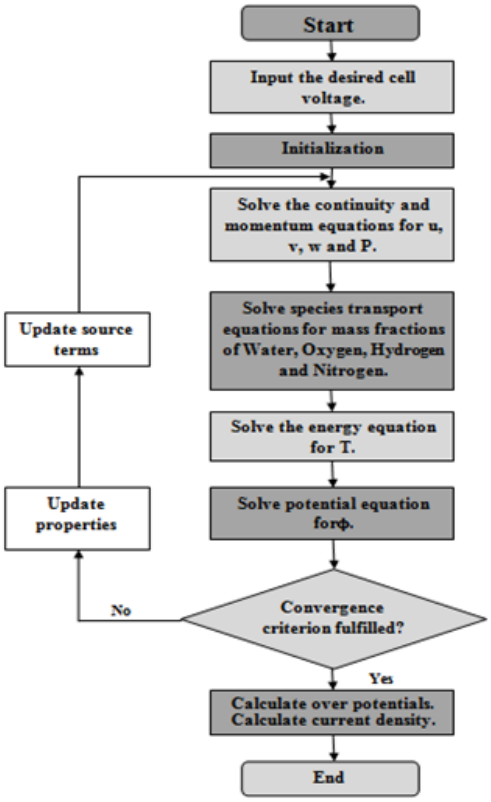

Fig. 4. The algorithm for numerical simulation in proton exchange membrane fuel cell.

5. Results and discussion

To validate the numerical simulation model used in the present study, the polarization curves were compared with the experimental data presented by Al-Baghdadi et al for the straight channel [19]. Polarization curve of conventional model is shown in Figure 5. This curve signifies excellent agreement between numerical model and experimental data which verifies using the present simulation. It is worth of explaining Fig. 5

in more detail, there is a no agreement between the numerical simulation results and experimental

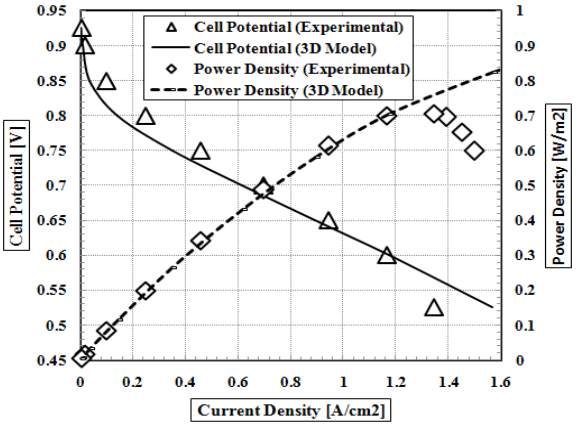

Fig. 5. Comparison of polarization curve of model with experimental data.

data at the high current density zone. This fact is the result of the neglecting liquid water. Moreover, the water formed in the catalyst layer is in the vapor phase (in numerical simulation). In fact, liquid water fills the pores of the catalyst and gas diffusion layers and does not let the oxygen molecules transfer to the catalyst layer easily and leads to species losses and therefore the cell faces with less species. The power density curve for the simulation is added too. There is a constant relation between voltage, current density and the power of the fuel cell as P =V.I. Proposed models were chosen In order to improve conventional cell performance by improving the distribution of reactants over the gas diffusion layer with the same reactant flow rate and operation conditions. Parametric and operating conditions can be found in Table 1 and 2. [19]

The comparison of the cell performance proposed in this work with a conventional cell must be done via polarization curves that detrmine the priority of fuel cell. The Figure 6 revealed that case with annular shape produces more current density than the conventional geometry. At low voltage, which PEM cells are operated practically in this zone, proposed model has great effect on performance in comparison with high voltage which is partially

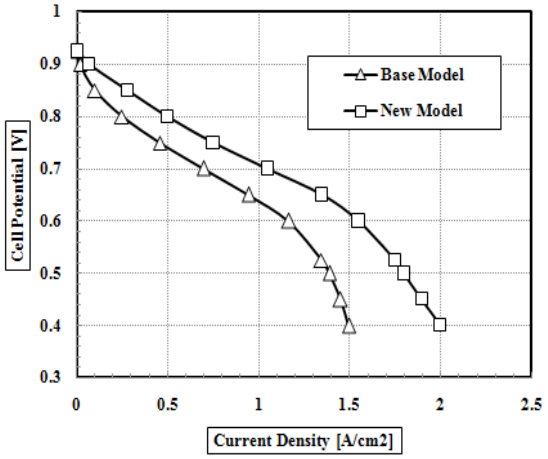

Fig. 6. The effect of novel geometry on the cell performance.

negligible.

Figure 7 presents hydrogen mass fraction at anode side for both 0.4 and 0.6 v. As it is shown gradually by going along the channel the amount of hydrogen decreases especially at low voltage strong reduction of hydrogen is sensed due to high consumption of species and lead to dead zones at out let region. The main reason for this phenomenon is diffusion of species from two sides along the channel which causes these dead zones. As observed in both fields, hydrogen distribution is very homogenous which help getting more output current density. Furthermore, the another priority of this model having two inlet instead of one in one cell which leads to better fuel supply for chemical reaction.

One of the main factors which affect the cell performance is oxygen. The profile of oxygen distribution at the membrane-cathode catalyst interface which is obtained in 0.4 and 0.6 voltage are shown in Figures 8. Figure demonstrates that by going along the channel the amount of oxygen decreases due to consumption. It is worth of explaining that at low voltage this consumption is more than high voltage which is obvious in the figure. As before mentioned, one of the benefits of this model which makes it volunteer of PEMFCs, having two inlet instead of one which leads to fuel cell does not feel any mass limitation problem. Fuel and oxygen concentration changes in the annular flow field are more than the

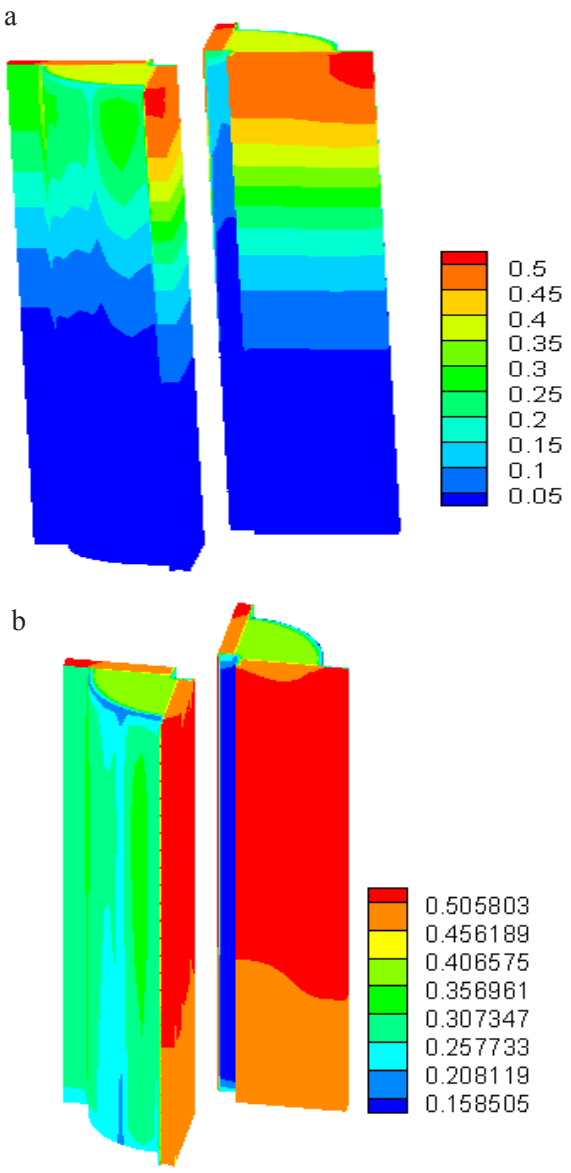

Fig. 7. Contours of hydrogen mass fraction at the catalyst layer and gas diffusion layer of anode for annular shape V=0.4 (a) and 0.6 (b).

conventional one. This could be attributed to the fact that more diffusion of species due to consumption from two sides in every channels (Fig. 3). Also the decrease in mass fraction of oxygen in cathode side is more than hydrogen in anode side due to water formation which blocks the porous area.

The water mass fraction distribution in the cell is presented in Figure 9 at V = 0.4 and 0.6 V for new geometry. It is clear that water management has important rule on performance of cell especially membrane for transporting protons. Additionally, any variation in water causes dehydration or flooding of PEMFC which must be controlled during working the fuel cell. As shown in Figure 9, water mass fraction increases along the channel due to the water production by oxygen consumption at the catalyst layer and the net water transferring due to electro-osmotic from the anode side toward the cathode side that causes decreases water magnitude at anode side especially at low voltage due to high rate of chemical reaction. It can be obtained in the downstream of channel the amount of water increases due to generating water molecules, which is uniform along the channel. Figure 10 presents the influence of annular flow simulation on the distribution of temperature at 0.6 cell voltage in the cross section of PEM fuel cell. It can be concluded that the maximum temperature of the cell is at the cathode catalyst layer that it is due to the maximum heat generation at the cathode side catalyst layer. Also Figure 10 shows a stagnation region around the bipolar plate and increment zone at the inlet region. This low value region in the shoulder zone is caused by heat conducting with bipolar plates which decreases the temperature. The slight temperature decrease along the channel is obvious; this is due to water formation along the channel. The least temperature happens at out let region because of presenting and forming more water and its distribution. Comparison of temperature distribution between two flow fields demonstate that there is lower temperature gradient (about 2 K) which could be attributed to high chemical reaction at low voltage.

Current density in the PEM fuel cell is shown in Fig. 11 for V= 0.4 and 0.6 respectively. Local current density is high at the reactant inlet and low at the outlet in both voltages. This is due to reduction of reactants concentration along the channels. It is benefit of explaining this phenomenon more, as the figure reveals at low voltage in the outlet channel the magnitude of this value decrease intensively due to water presence which blocked the GDL and interrupted the chemical reaction. Overall in this geometry local current density distribution shows very uniform and homogenous counters. It is clear that the current density is higher

a

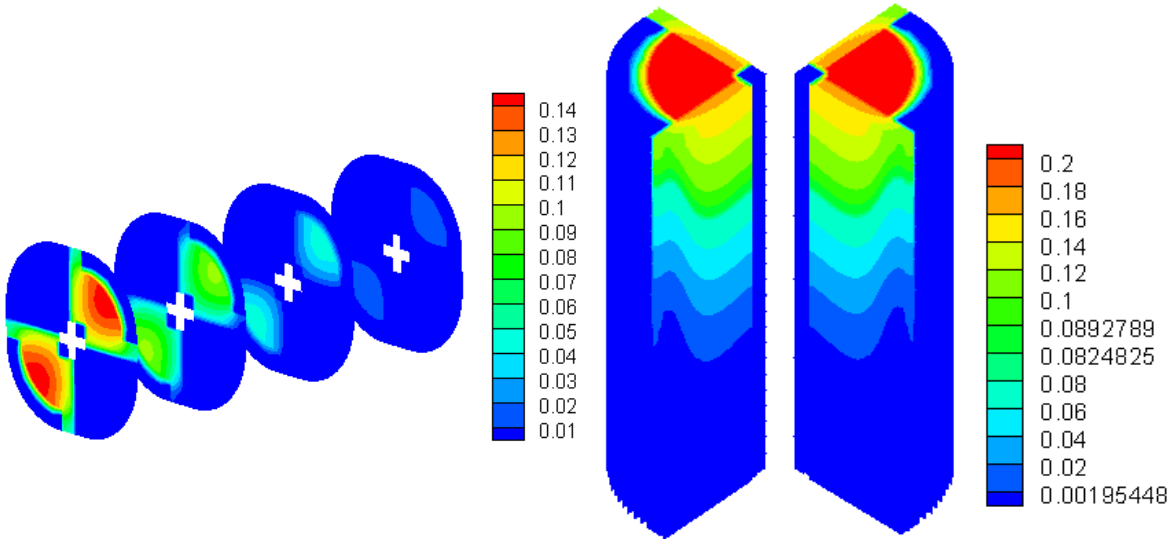

b

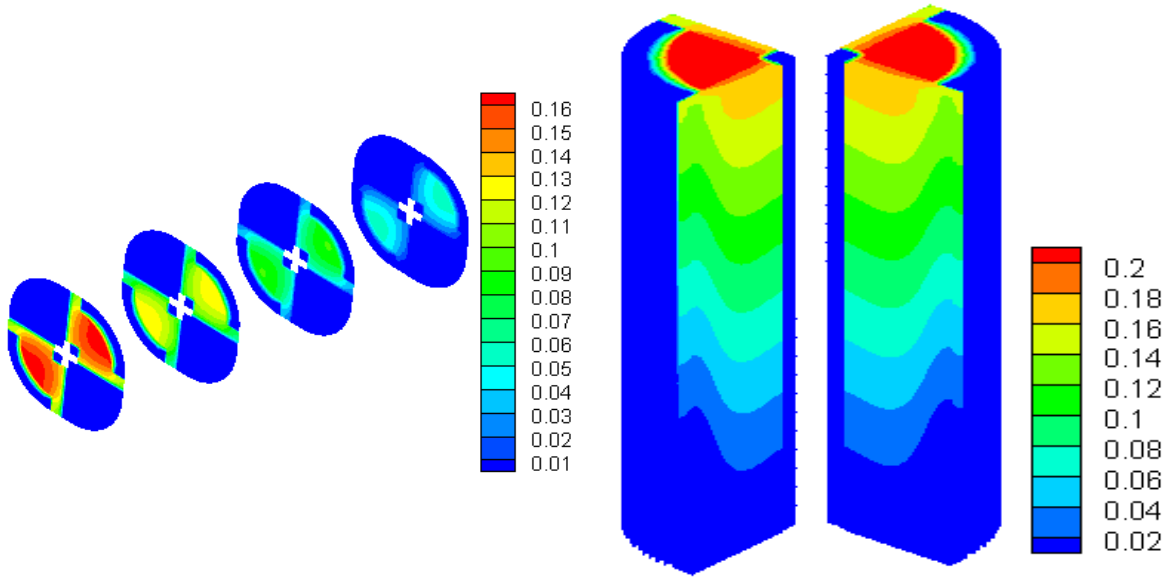

Fig. 8. Contours of oxygen mass fraction at the catalyst layer and gas diffusion layer of cathode annular model V=0.4(a), and 0.6 (b).

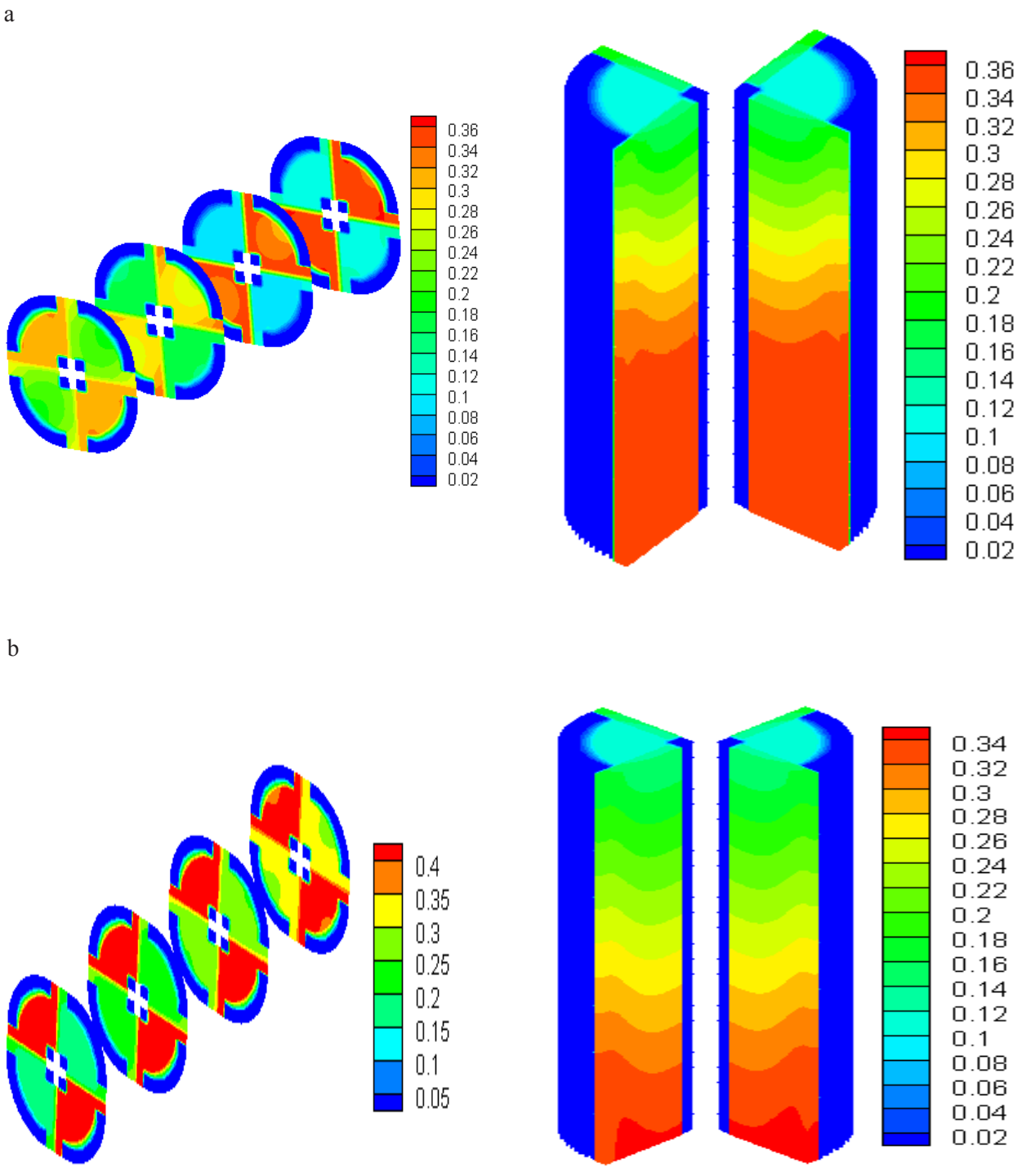

Fig. 9. Contours of water mole fraction at the catalyst layer and gas diffusion layer of cathode for V= 0.4 (a), and 0.6(b).

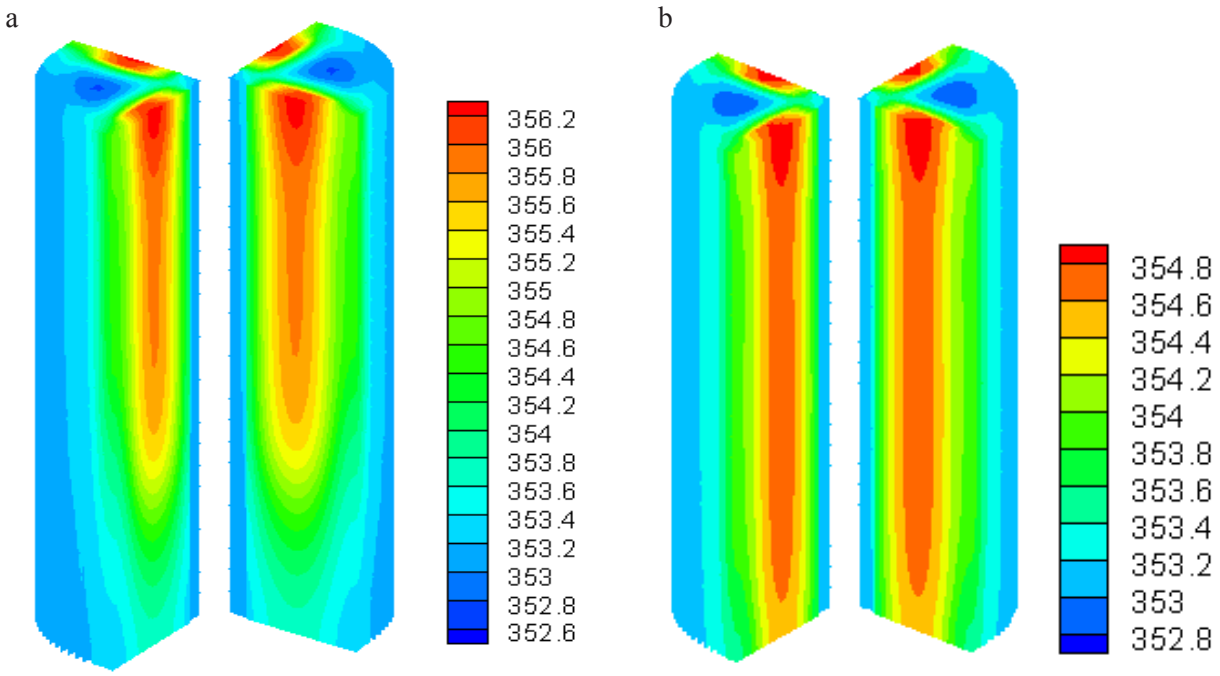

Fig. 10. Contours of Temperaure at the catalyst layer and gas diffusion layer of cathode for V= 0.4 (a) and 0.6 (b)v.

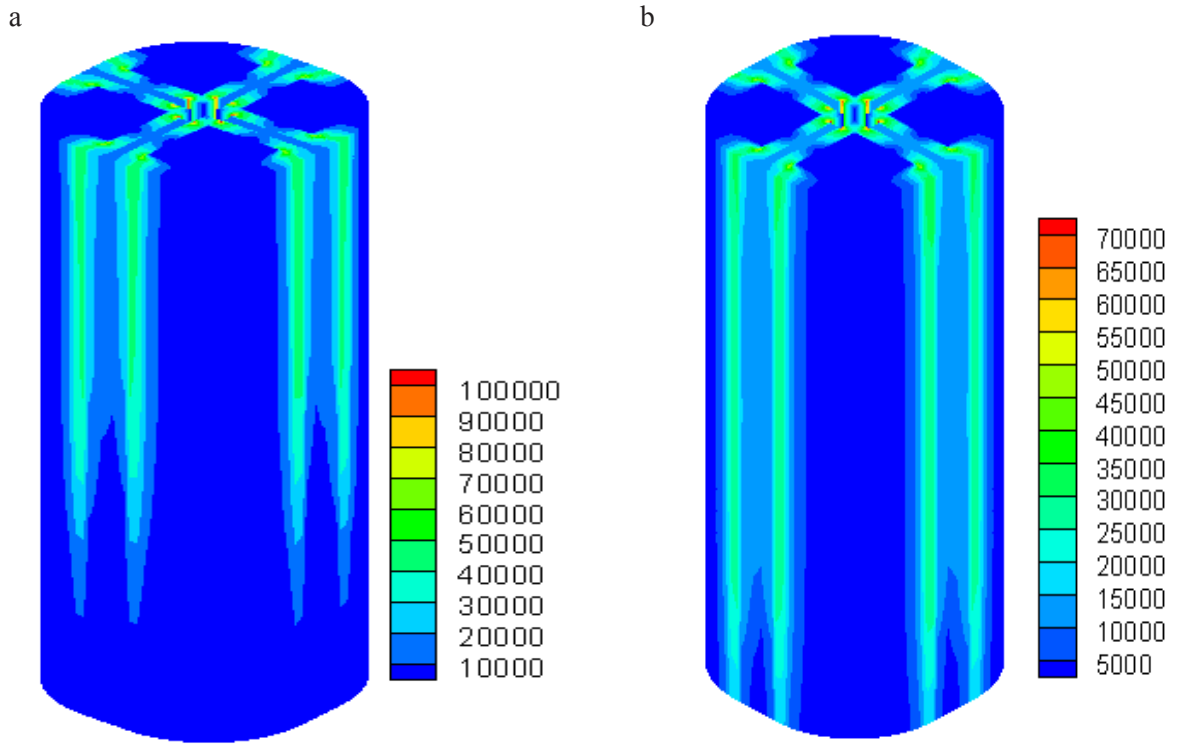

Fig. 11. Contours of Current density distribution of cathode for V= 0.4(a), and 0.6 v (b).

at the connections between GDL and bipolar which is the main way of output current density.

The effect of GDL thickness is presented in Fig. 12. As shown in the picture, by increasing the GDL thickness up to specific value the slight increase in current density will be resulted but more than this value this phenomenon will be reversed. This could be attributed to the decreasing the inlet surface and

more penetration and difuusion in the MEA but more increasing the thickness, cause to more accuumulation of water and species losses in annular geometry.

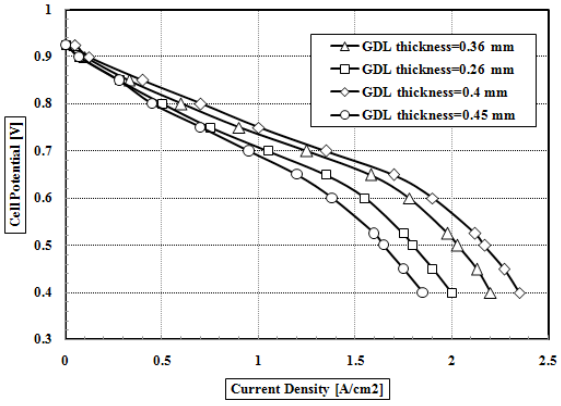

Fig. 12. Effect of GDL thickness on the cell performance.

6. Conclusion

In the present research, a three-dimensional computational fluid dynamics model of polymer electrolyte membrane fuel cell with annular flow channel has been conducted in order to improve the cell performance. The simulated model was based on solving the conservation equations for membrane and flow channels which is discretized on the base of finite volume scheme. One-phase and non-isothermal assumption were applied. The introduced cell consist of different novelties, such as the way in which reactant gases are supplied to the flow field, the design of the flow field geometry for both anode and cathode and the membrane electrode assembly design. The following conclusions are drawn:

1. Simulation results were compared with the experimental data and signified good agreement between the model and experimental data.
2. An important result in this introduced model is obtaining intensively higher current density. It is found that the geometry presented in this work is capable of producing large current densities despite of having shorter lenght and less occupied volume up to 40%.
3. The hydrogen mass fraction gradually decreases due to consumption from two sides in every channel especially by decreasing the voltage. Furthermore, supplying gases from two inlet cause to decreasing species losses.
4. The membrane new geometry in every channels leads to higher consumption of oxygen in cathode channel and uniform distribution.
5. A uniform temperature distribution can be reached by applying this model.
6. The maximum of local current density obtained at inlet area and the magnitude of current density decreased along the channel due to water formation and less value of species.
7. The result of simulation revealed that GDL thickness has constructive role on the cell performance which at specific thickness will have signigicant impact.

Acknowledgment

The financial support of the Renewable Energy Organization of Iran (SUNA) is gratefully acknowledged.

Nomenclature:

a	Water activity
C	Molar concentration (mol/m^3)
D	Mass diffusion coefficient (m^2/s)
F	Faraday constant (C/mol)
I	Local current density (A/m^2)
J	Exchange current density (A/m^2)
K	Permeability (m^2)
M	Molecular weight (kg/mol)
n_d	Electro-osmotic drag coefficient
P	Pressure (Pa)
R	Universal gas constant (J/mol-K)
T	Temperature (K)
t	Thickness
V	Cell voltage
V_{oc}	Open-circuit voltage
W	Width
X	Mole fraction

Greek Letters:

α	Water transfer coefficient
ε_{eff}	Effective porosity
ρ	Density (kg/m^3)
μ	Viscosity (kg/m-s)
σ_e	Membrane conductivity (1/ohm-m)
λ	Water content in the membrane
ζ	Stoichiometric ratio
η	Over potential (v)
λ_{eff}	Effective thermal conductivity (w/m-k)

Subscripts and Superscripts:

a	Anode
c	Cathode
cl	Catalyst
GDl	Gas diffusion layer
ch	Channel
k	Chemical species
m	Membrane
MEA	Membrane electrolyte assembly
ref	Reference value
sat	saturated
w	Water

7. References

[1] Torkavannejad A., Pesteei M., Ramin F., Ahmadi, N., "Effect of innovative channel geometry and its effect o species distribution in PEMFC", journal of renewable energy and environment, Volume 1 - 1, January 2014, pp. 20-31

[2] Torkavannejad A,, Pesteei M., Khalilian M., Ramin F., "EFFECT OF DEFLECTED MEMBRANE ELECTRODE ASSEMBLY ON SPECIES DISTRIBUTION IN PEMFC", International Journal of Engineering (IJE), (March 2015), Vol. 28, No. 3 460-469.

[3]. Ahmadi N., Rezazadeh S., Mirzaee I. and Pourmahmoud N., "Three-dimensional computational fluid dynamic analysis of the conventional PEM fuel cell and investigation of prominent gas diffusion layers effect". Journal of Mechanical Science and Technology. 2012, 12(8), 1-11.

[4] Imanmehr S., Pourmahmoud N, Parametric Study of Bipolar Plate Structural Parameters on the Performance of Proton Exchange Membrane Fuel Cell, J. Fuel Cell Sci. Technology.ASME, 2012, 9 pages.

[5] Pourmahmoud N., Rezazadeh S., Mirzaee I. and S. Motaleb Faed, "A Computational Study of a Three-dimensional Proton Exchange Membrane Fuel Cell (PEMFC) with Conventional and Deflected Membrane Electrode", 2012, 26 (9), 2959-2968.

[6] Pourmahmoud N. , Rezazadeh S., Mirzaee I., heidarpoor v., "Three-dimensional numerical analysis of proton exchange membrane fuel cell, Journal of Mechanical Science and Technology", 2011, 25 (10): 2665-2673.

[7] Wang X. D., Huang Y. X., Cheng C. H., Jang J. Y., Lee D. J., Yan, W. M., and Su, A., "An Inverse Geometry Design Problem for Optimization of Single Serpentine Flow Field of PEM Fuel Cell," Int. J. Hydrogen Energy, 2010, 35:4247–4257.

[8] Wang X. D., Zhang X. X., Liu T., Duan, Y. Y., Yan W. M., and Lee, D. J., "Channel Geometry Effect for Proton Exchange Membrane Fuel Cell With Serpentine Flow Field Using a Three-Dimensional Two-Phase Model", ASME J. Fuel Cell Sci. Technol., 2010, 7, p. 051019.

[9] Ramos- Alvarado, B., Hernandez- Guerrero, A., Juarez-Robles, D.,Li, L., "Numerical investigation of the performance of symmetric flow distributors as flow channels for PEM fuel cells" international journal of hydrogen energy , 2012, 37:436-448.

[10] Chen, Y. S., and Peng, H., 2011, "Predicting Current Density Distribution of Proton Exchange Membrane Fuel Cells With Different Flow Field Designs," J. Power Sources, 196, pp. 1992–2004.

[11] Cano-Andrade S., Hernandez-Guerrero A., M.R. von

Spakovsky , C.E. Damian-Ascencio, J.C. Rubio-Arana, "Current density and polarization curves for radial flow field patterns applied to PEMFCs (Proton Exchange Membrane Fuel Cells)", Energy, (2010), 35: 920–927.

[12] Friess B.R., Hoorfar M.,"Development of a novel radial cathode flow field for PEMFC", International Journal of hydrogen energy, 2012, 37: 7719-7729.

[13] Surajudeen Olanrewaju Obayopo, "Performance Enhancement in Proton Exchange Membrane Fuel Cell-Numerical Modeling and Optimisation", PhD thesis, University of Pretoria, 2012.

[14] "Three Dimensional Analysis of a PEM Fuel Cell with the Shape of a Fermat Spiral for the Flow Channel Configuration", Proceedings of IMECE2008, ASME International Mechanical Engineering Congress and Exposition October 31-November 6, 2008, Boston, Massachusetts, USA.

[15] Brooks Regan Friess, "Development of Radial Flow Channel for Improved Water and Gas Management of Cathode Flow Field in Polymer Electrolyte Membrane Fuel Cell", Masters of Applied Science Thesis, University of British Columbia, 2010.

[16] Tiss F., Chouikh R., Guizani A., "A numerical investigation of reactants transport in a PEM fuel cell with partially blocked gas channel", Energy Conversion and management, 2014, 80:32-38.

[17] Walczyk D. F., and Sangra J. S., 2010, "A Feasibility Study of Ribbon Architecture for PEM Fuel Cells," ASME J. Fuel Cell Sci. Technol.,2010, 23: 123-189.

[18] Khazaee I., Ghazikhani M., "Three-Dimensional Modeling and Development of the New Geometry PEM Fuel Cell, Arab J Sci Eng"., 2013,38: 1551–1564.

[19] Maher A.R. Sadiq Al-Baghdadi, Haroun A.K. Shahad Al-Janabi, "Parametric and optimization study of a PEM fuel cell performance using three-dimensional computational fluid dynamics model", Renewable Energy, 2007, 32 : 1077–1101.